Glycogen degrading activities of catalytic domains of α-amylase and α-amylase-pullulanase enzymes conserved in *Gardnerella* spp. from the vaginal microbiome

Pashupati Bhandari[1], Jeffrey Tingley[2], D. Wade Abbott[2] and Janet E. Hill[1,*]

[1]Department of Veterinary Microbiology, University of Saskatchewan, Saskatoon, Saskatchewan, Canada

[2]Lethbridge Research and Development Centre, Agriculture and Agri-Food Canada, Lethbridge, Alberta, Canada

*Correspondence: Janet.Hill@usask.ca

Abstract

Gardnerella spp. are associated with bacterial vaginosis, in which normally dominant lactobacilli are replaced with facultative and anaerobic bacteria including *Gardnerella* spp. Co-occurrence of multiple species of *Gardnerella* is common in the vagina and competition for nutrients such as glycogen likely contributes to the differential abundances of *Gardnerella* spp. Glycogen must be digested into smaller components for uptake; a process that depends on the combined action of glycogen degrading enzymes. In this study, the ability of culture supernatants of 15 isolates of *Gardnerella* spp. to produce glucose, maltose, maltotriose and maltotetraose from glycogen was demonstrated. Carbohydrate active enzymes were identified bioinformatically in *Gardnerella* proteomes using dbCAN2. Identified proteins included a single domain α-amylase (EC 3.2.1.1) (encoded by all 15 isolates) and an α-amylase-pullulanase (EC 3.2.1.41) containing amylase, carbohydrate binding modules and pullulanase domains (14/15 isolates). To verify the sequence-based functional predictions, the amylase and pullulanase domains of the α-amylase-pullulanase, and the single domain α-amylase were each produced in *E. coli*. The α-amylase domain from the α-amylase-pullulanase released maltose, maltotriose and maltotetraose from glycogen, and the pullulanase domain released maltotriose from pullulan and maltose from glycogen, demonstrating that the *Gardnerella* α-amylase-pullulanase is capable of hydrolyzing α-1,4 and α-1,6 glycosidic bonds. Similarly, the single domain α-amylase protein also produced maltose, maltotriose and maltotetraose from glycogen. Our findings show that *Gardnerella* spp. produce extracellular amylase enzymes as 'public goods' that can digest glycogen into maltose, maltotriose and maltotetraose that can be used by the vaginal microbiota.

Importance

Increased abundance of *Gardnerella* spp. is a diagnostic characteristic of bacterial vaginosis, an imbalance in the human vaginal microbiome associated with troubling symptoms, and negative reproductive health outcomes, including increased transmission of sexually transmitted infections and preterm birth. Competition for nutrients is likely an important factor in causing dramatic shifts in the vaginal microbial community but little is known about the contribution of bacterial enzymes to the metabolism of glycogen, a major food source available to vaginal bacteria. The significance of our research is characterizing the activity of enzymes conserved in *Gardnerella* species that contribute to the ability of these bacteria to utilize glycogen.

Introduction

Gardnerella spp. are associated with bacterial vaginosis (BV), a condition characterized by the replacement of the usually dominant *Lactobacillus* community with a mixture of facultative and anaerobic bacteria including *Gardnerella* spp. (1). BV is characterized by thin, white to greyish discharge and unpleased 'fishy' vaginal odor, however a large majority of women diagnosed with BV do not have symptoms (2). Phenotypic diversity among *Gardnerella* spp. may explain why they are found in women presenting clinical signs of bacterial vaginosis and in asymptomatic or BV negative women (3). The genus *Gardnerella* has been classified into four different species and at least 13 "genome species" (4). Co-occurrence of multiple *Gardnerella* species in the vaginal environment is common, and different species are dominant in different women (5). Given the potentially different roles of *Gardnerella* species in the vaginal microbiome, understanding the factors contributing to their population structure is important. Previous work has shown that interactions in co-cultures of *Gardnerella* spp. are typical of a "scramble" competition (6). In scramble competition, one competitor outgrows others through its superior

60 ability to use shared resources such as nutrients (7). Competition for nutrients could be an
61 important factor contributing to the differential abundances of *Gardnerella* spp. in the vaginal
62 microbiome.

63 Glycogen is an abundant carbon and energy source available to the vaginal microbiota
64 including *Gardnerella*. Glycogen is a glucose homopolysaccharide comprising linear α-1,4 linked
65 glucose with α-1,6 branch points occurring approximately at every 8-13 residues to from a highly
66 branched and complex structure. The sizes of glycogen molecules and branching patterns can vary
67 based on the glycogen source (8). In the vagina, glycogen accumulates inside vaginal epithelial
68 cells under the influence of estrogen (9) and is released into the vaginal lumen through the activity
69 of bacterial cytolysins and/or lactic acid mediated acidosis (10). The amount of free glycogen in
70 vaginal fluid can range from undetectable to 32 μg/ml (11).

71 Glycogen must be digested into smaller products for uptake into bacterial cells. This
72 complex and multistep process requires the combined action of enzymes collectively known as
73 glycogen degrading enzymes. The majority of Glycogen degrading bacterial amylases belong to
74 the glycosyl hydrolase (GH) class within family 13 in the classification of carbohydrate active
75 enzymes. GH13 enzymes are further classified into more than 40 subfamilies based on their
76 structure and substrate specificity (12). Previous studies have shown the presence and activity of
77 human and/or bacterial amylases in vaginal fluid (13, 14) but the specific contribution of
78 *Gardnerella* spp. to glycogen digestion is not clear.

79 This study aimed to assess the glycogen digestion ability of *Gardnerella* spp. isolated from
80 the vaginal microbiome and to determine the distribution of extracellular glycogen degrading
81 enzymes among different species. In addition, we aimed to biochemically characterize the
82 activities of the predicted functional domains of extracellular glycogen degrading amylase

83 enzymes identified. Our findings showed that *Gardnerella* spp. have α-amylase and α-amylase-
84 pullulanase enzymes which can digest glycogen into maltose and other oligosaccharides.
85
86 **Methods**
87 ***Gardnerella* isolates**
88 Isolates of *Gardnerella* used in this study were from a previously described culture
89 collection (15) and included a total of 15 *Gardnerella* spp. isolates [three representative strains
90 each from *G. leopoldii* (GH005, VN003 & NR017), *G. piotii* (VN002, GH007 & GH020), *G.*
91 *vaginalis* (NR038, NR001 & NR039) and *G. swidsinskii* (NR016, NR021 & NR020), two isolates
92 from *Gardnerella* genome sp. 3 (NR026 & N170) and one from unknown genome species (NR047,
93 subgroup D based on cpn60 classification system). Whole genome sequence data for all isolates
94 were retrieved from NCBI BioProject Accession PRJNA394757.
95 **Amylase activity assay**
96 Amylase activity of *Gardnerella* isolates was assessed using a glycogen iodine test (16).
97 Isolates were revived from -80°C storage on Columbia blood agar plates containing 5% sheep
98 blood, and incubated anaerobically using the GasPak system (BD, USA) at 37°C for 48 hours.
99 Isolated colonies were transferred into modified NYCIII broth (obtained by replacing horse serum
100 with bovine serum and omitting glucose in NYCIII media) and incubated anaerobically for 24
101 hours at 37°C. Overnight broth cultures were centrifuged at 10,000 × *g* for 10 mins and the cell-
102 free supernatant was passed through a 0.45 µm filter. Filtered supernatant (10 µL) was spotted on
103 to a 1% (w/v) glycogen (Bovine liver glycogen, Sigma) agar plate and incubated anaerobically at
104 37°C for 24 hours. Filtered supernatant was also streaked on Columbia sheep blood agar to confirm
105 sterility. Plates were flooded with 1% (w/v) Lugol's iodine solution to detect evidence of amylase

106 activity. α-amylase from *Bacillus licheniformis* (0.05 mg/ml) (Sigma-Aldrich, Oakville, ON, CAT
107 No. A455) and modified NYCIII broth were used as positive and negative controls respectively.
108 Activity of cell culture supernatants on glycogen was assessed by incubating culture
109 supernatants with glycogen and examining the products. Briefly, 20 µl of culture supernatant was
110 added to 180 µl of 0.1% bovine liver glycogen in 50 mM sodium phosphate buffer, pH 7.0 and
111 incubated at 37ºC. Aliquots (50 µl) of the reaction mixture were collected at 24 h and were frozen
112 immediately until analysis by thin layer chromatography (TLC) and high-performance anion
113 exchange chromatography with pulsed amperometric detection (HPAEC-PAD). TLC was
114 performed on silica plates in a 1-butanol, acetic acid and distilled water (2:1:1 [vol:vol:vol]) mobile
115 phase and stained using 0.3% of N-napthyl ethylenediamine dihydrochloaride (Sigma) as
116 described previously (17). HPAEC-PAD samples were first precipitated with 80% ethanol to
117 remove large polysaccharides and diluted (to 1:20 for G5 and maltodextrin or 1:10 for glycogen)
118 and resolved on a Dionex PA20 column in a mobile phase of 30 mM NaOH and gradient of 10
119 mM to 120 mM sodium acetate over 40 min at a flow rate of 0.5 ml min^{-1}. Data were analyzed
120 using Chromeleon v6.80 chromatography data system software.
121 **Identification of the carbohydrate active enzymes (CAZyme)**
122 The *Gardnerella* proteomes, predicted from the RAST annotation, were uploaded into the
123 dbCAN2 webserver (18). All three available domain prediction tools (HMMER, eCAMI and
124 DIAMOND) were used to annotate the carbohydrate active domain(s) in protein sequences. The
125 dbCAN2 uses SignalP to predict whether a signal peptide is present or absent in the protein in
126 which each carbohydrate active domain is located. To identify secreted glycogen degrading
127 glycosyl hydrolases, dbCAN2 output was filtered to include only GH13 domain(s) associated with

128 signal peptide. TMHMM 2.0 (19) and LocateP (20) were used to predict transmembrane and cell-
129 wall anchored domains respectively.

130 **Phylogenetic analysis of GH13_32 amylase domains**

131 Domains belonging to subfamily 32 within the family 13 of glycosyl hydrolases class are
132 referred to as GH13_32 amylase domains. Amino acid sequences corresponding to the GH13_32
133 amylase domain were extracted from predicted extracellular glycosyl hydrolases of all study
134 isolates and four *Gardnerella* reference strains [(*G. leopoldii*, (CP029984)), *G. piotii*
135 (QJUV00000000), *G. vaginalis* (QJUZ00000000) and *G. swidsinskii* (QJVB00000000)](4).
136 Multiple-sequence alignments were performed using CLUSTALw and a neighbour joining
137 consensus tree was built in Geneious prime version 2022.1.1 (https://www.geneious.com). The
138 final tree was visualized using Figtree (v1.4.4).

139 To identify the conserved catalytic residues in GH13_32 domains, amino acid sequences
140 of representative GH13_32 domains of *G. leopoldii* NR017 were combined with GH13_32 domain
141 sequences from functionally characterized α-amylases [*Pseudoalteromonas haloplanktis* A23
142 (CAA41481.1) and *Streptomyces venezuelae* ATCC 15068 (AAB36561.1)] and amylopullulanase
143 [*Bifidobacterium breve* UCC2003 (AAY89038.1)] deposited in the CAZy database. Sequences
144 were aligned using CLUSTALw and alignments were visualized in ESPript (21).

145 **Expression and purification of α-amylase and pullulanase domains from α-amylase-**
146 **pullulanase**

147 To characterize activities of the amylase and pullulanase domains of the α-amylase-
148 pullulanase, *G. leopoldii* (NR017) was chosen as a representative isolate. Genomic DNA was
149 extracted from *G. leopoldii* NR017 using a modified salting out procedure. Primers
150 (Supplementary Table 1) were designed to amplify the nucleotide sequences encoding the

151 predicted α-amylase (corresponding to amino acids 74-350 of Genbank Accession RFT33565) and
152 pullulanase (corresponding to amino acids 1141-1462 of Genbank Accession RFT33565) domains
153 of the NR017 α-amylase-pullulanase gene along with 30 additional flanking nucleotides each on
154 the 5' and 3' ends. PCR was carried out in PCR buffer (0.2 M Tris-HCl [pH 8.4], 0.5 M KCl), a
155 200 mM concentration of each deoxynucleoside triphosphate (dNTP), 2.5 mM $MgCl_2$, a 400 nM
156 concentration of each primer (α-amylase: JH0810-F & JH0811-R, or pullulanase: JH0812-F &
157 JH0813-R), 1 U/reaction of Platinum Taq DNA polymerase high-fidelity (5 U/ml in 50% glycerol,
158 20 mM Tris-HCl, 40 mM NaCl, 0.1 mM EDTA, and stabilizers) (Life Technologies), and 2 μl of
159 template DNA, in a final volume of 50 μl. PCR was performed with the following parameters:
160 initial denaturation at 94°C for 3 min, 40 cycles of denaturation at 94°C for 15 s, annealing at 60°C
161 for 15 s, and extension at 72°C for 1 min (for α-amylase domain) or 1.5 min (for pullulanase
162 domain), and final extension at 72°C for 3 min. Purified PCR products were digested with *Bam*HI
163 and *Kpn*I and ligated into expression vector pQE-80L treated with the same restriction
164 endonucleases. The pQE-80L+amylase domain plasmid (henceforth referred to as pQE80L-AMY)
165 was used to transform chemically competent *E. coli* Rosetta DE3 cells (Novagen, Sigma-Aldrich),
166 and the pQE-80L+pullulanase domain plasmid (henceforth referred to as pQE80L-PULL) was
167 used to transform One Shot TOP10 chemically competent *E. coli* cells (Invitrogen, Carlsbad, CA).
168 Insertion of amylase and pullulanase domain encoding sequences in frame with the N-terminal
169 His-tag was confirmed by sequencing of the purified plasmid.

170 *E. coli* Rosetta cells containing pQE80L-AMY were grown in 800 ml of LB broth
171 containing ampicillin (100 μg/ml) and chloramphenicol (25 μg/ml) whereas *E. coli* Top10 cells
172 containing pQE80L-PULL were grown in same volume of LB broth with ampicillin (100 μg/ml)
173 only. Once the culture reached an optical density at 600 nm (OD_{600}) of 0.4 - 0.6, protein expression

174 was induced with 0.5 mM IPTG. After 4 h of incubation at 37°C with shaking at 200 rpm, cells
175 were harvested by centrifugation at 8500 × *g* for 20 min at 4°C and pellets were stored at -20°C
176 until further processing. Proteins were solubilized using anionic detergent as described previously
177 (22) with a slight modification during sonication (6 min total run time, 2 min on, 1 min off at 4°C).
178 Eluted proteins were dialyzed against 1 × PBS (pH 7.4) at 4°C using a semipermeable membrane
179 with cut-off size 12 kDa for 24 - 48 hours. The diluted proteins were concentrated using a 30 kDa
180 molecular weight cut-off protein concentrator (Thermo Fisher Scientific). Final protein
181 concentration was measured using a Nanodrop spectrophotometer before storing at -20°C.

182 **Expression and purification of single amylase domain containing α-amylase**

183 A codon-optimized DNA construct corresponding to the full-length open reading frame of
184 single domain α-amylase from *G. leopoldii* NR017 (RFT33564.1) was synthesized and a region
185 encoding amino acids 58-519 (excluding N-terminal signal peptide and C-terminal transmembrane
186 domain) was amplified using JH0857 and JH0858 primers (Supplementary Table 1). The 1463 bp
187 product was ligated into *Mfe*I *and Hind*III digested pET41a+ vector to express as a N-terminal
188 GST-His tag fusion protein (79.9 kDa). The recombinant plasmid (pET41a+CO-AMY) was used
189 to transform chemically competent *E. coli* DH5α cells. Presence of the insert in frame with the N-
190 terminal GST-His-tag was confirmed by Sanger sequencing of the purified plasmid.

191 Purified recombinant plasmid (pET41a+CO-AMY) was used to transform *E. coli*
192 BL21DE3 cells for protein production. *E. coli* BL21DE3 cells containing recombinant plasmid
193 were grown in 1.8 L of LB broth containing kanamycin (30 μg/ml). When culture reached to
194 optical density OD_{600} 0.4 - 0.6, IPTG was added to a final concentration of 0.5 mM to induce
195 protein expression at 37ºC for 4 hours with shaking at 200 rpm. Cells were harvested by
196 centrifugation at 8500 × *g* for 20 min. Expressed protein was solubilized using anionic detergent

197 as described previously (22) with slight modification of the sonication protocol (80% duty cycle,
198 8 minutes total run time, 10 secs on, 5 secs off). The recombinant amylase protein was purified
199 using a nickel column. Eluted proteins were dialyzed against 1× PBS (pH 7.4) at 4°C overnight
200 using a semipermeable membrane of cut-off size 12 kDa, and dialyzed protein was concentrated
201 using a 30 kDa molecular weight cut-off protein concentrator (Thermo Fisher Scientific). Final
202 protein concentration was measured using a Nanodrop spectrophotometer before storing at -20°C.
203 The region encoding the GST and 6xHis tags was expressed from empty pET41a vector in
204 *E. coli* BL21DE3 cells and was purified using Ni-affinity chromatography for use as a negative
205 control in activity experiments.

206 **Enzyme activity on different substrates**

207 The activity of purified enzymes was tested by incubating purified enzymes with different
208 substrates. Briefly, 250 µl of the purified amylase domain (22.3 µM) or α-amylase (13.0 µM) was
209 incubated with 1% glycogen, maltodextrin (dextrose equivalent 13-17) or maltopentose while
210 purified pullulanase (25.3 µM) was incubated with 1% maltotriose, maltotetraose, maltopentose,
211 pullulan and glycogen. To test the combined activity of α-amylase and pullulanase domains, an
212 equimolar (25.3 µM) mixtures of both enzymes were incubated with glycogen (1%). All substrates
213 were prepared in 50 mM sodium phosphate buffer at pH 6.0. Enzyme substrate reaction mixtures
214 were incubated at 37ºC for 24 h and stored at -20°C until further analysis by TLC or HPAEC-PAD
215 as described above.

216

217 **Results**

218 **Amylase activity of *Gardnerella* culture supernatants**

219 No growth was observed from filtered culture supernatants, confirming their sterility.
220 Supernatants of all 15 isolates showed amylase activity in the agar plate assay (Figure 1). Cell-free
221 culture supernatants of 14 isolates produced glucose, maltose, maltotriose and maltotetraose from
222 glycogen while glucose was the only product detected from N170 supernatant (*Gardnerella*
223 genome sp. 3, GS3-2) (Figure 2).

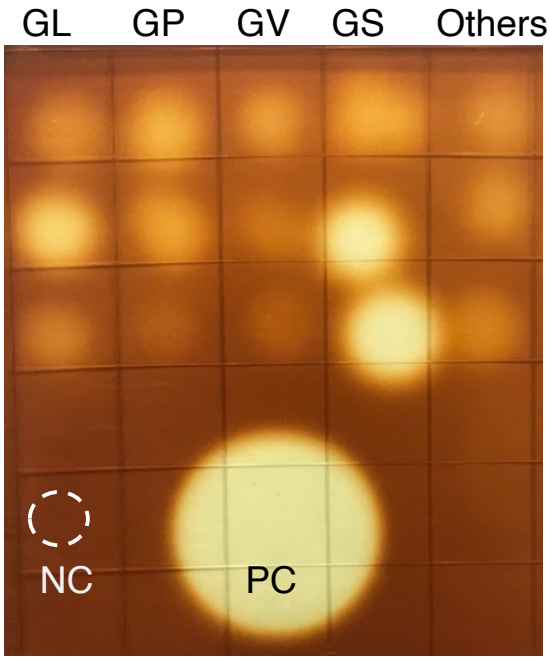

224

225 Figure 1: Amylase activity of cell free culture supernatants on glycogen agar. Each spot represents
226 one isolate and a total of 15 different isolates, three each from GL: *G. leopoldii*, GP: *G. piotii*,
227 GV: *G. vaginalis*, GS: *G. swidsinskii* and others [two isolates from *Gardnerella* genome sp. 3 (top
228 & middle) and one isolate from unknown genome species (bottom) (corresponds to the subgroup
229 D based on cpn60 classification system)] are shown. NC: mNYC, PC: *B. licheniformis* amylase
230 (0.05 mg/ml).
231

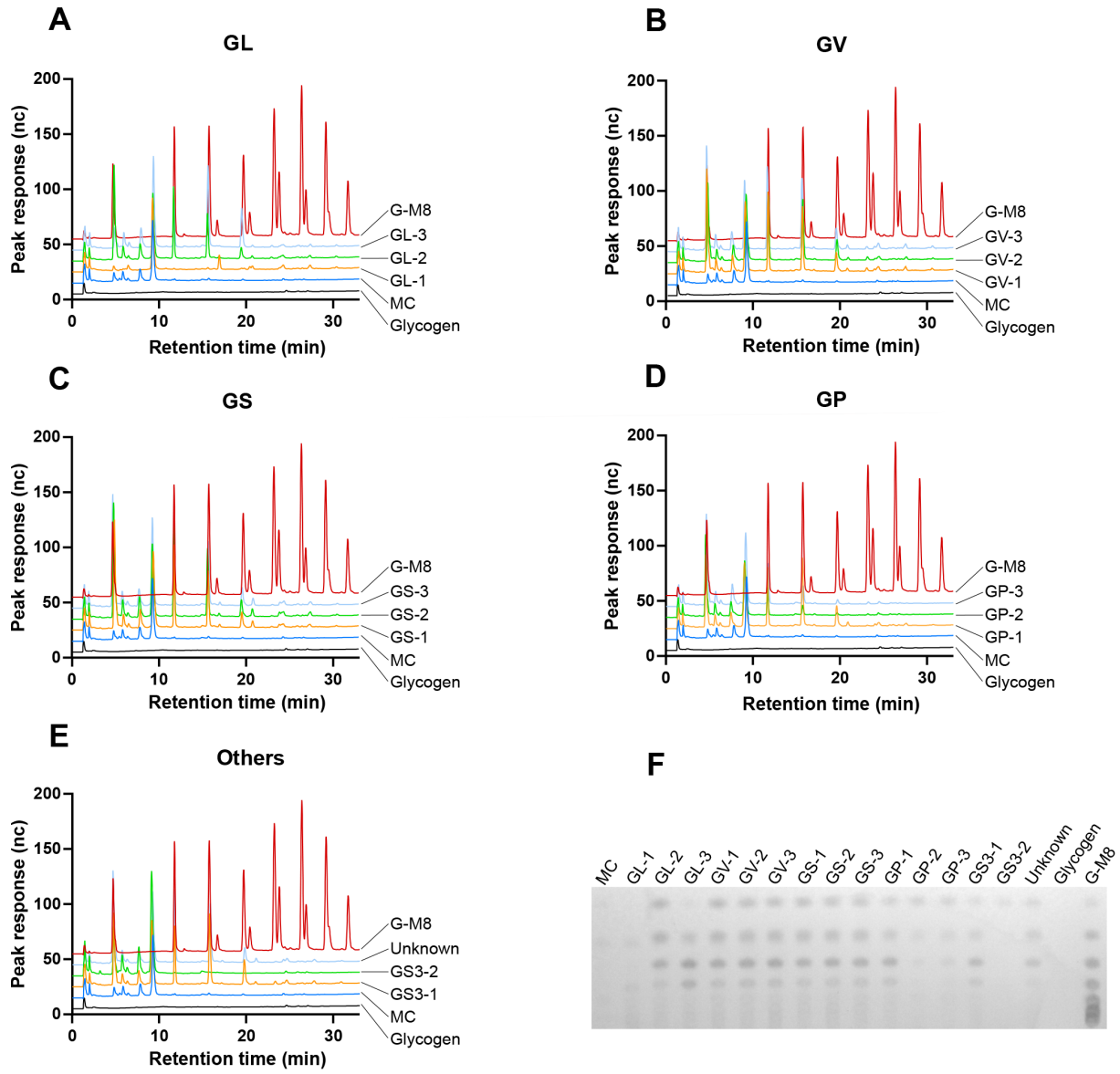

Figure 2: Identification of glycogen breakdown products produced after 24 h by culture supernatants of 15 *Gardnerella* isolates by HPAEC-PAD (A-E) and TLC (F). GL: *G. leopoldii*, GV: *G. vaginalis*, GS: *G. swidsinskii*, GP, *G. piotii*, and others [two isolates from *Gardnerella* genome sp. 3 (top & middle) and one isolate from unknown genome species (bottom) (corresponds to the subgroup D based on cpn60 classification system)], MC: media control, G-M8: glucose to maltooctaose standards.

241 **Identification of genes encoding carbohydrate active enzymes in *Gardnerella* genomes**

242 Out of 20,017 predicted protein sequences from 15 isolates uploaded into the dbCAN2
243 webserver, 886 sequences had at least one carbohydrate active domain. Results were filtered to
244 include only glycosyl hydrolase (GH) domains associated with a signal peptide. Only 52/836
245 sequences identified as belonging to the GH class had an associated signal peptide. Results were
246 further filtered to identify predicted extracellular glycogen degrading enzymes (protein containing
247 at least one GH13 domain associated with signal peptide), resulting in identification of 29
248 sequences.

249 A multidomain enzyme containing an N-terminal α-amylase domain (GH13_32), followed
250 by 2 - 4 carbohydrate binding modules (CBM, of types CBM25, CBM41 or CBM48) and a C-
251 terminal pullulanase domain (GH13_14) was identified in all isolates except N170. This enzyme
252 also included an N-terminal signal peptide domain, and a potential sortase sorting signal including
253 an LPxTG motif (Figure 3A). This multidomain enzyme is traditionally referred to as Type II
254 amylopullulanase, however, recently it has been suggested that these enzymes are more
255 appropriately classified as Type II α-amylase-pullulanase (23) and so the term 'α-amylase-
256 pullulanase' is used throughout this paper. The domain organization of *G. leopoldii* NR017 α-
257 amylase-pullulanase (RFT33565.1) is shown in Figure 3A. Similarly, a single α-amylase
258 (GH13_32) domain containing α-amylase enzyme with an N-terminal signal peptide and a C-
259 terminal transmembrane domain was identified in all 15 isolates (NR017 accession number
260 RFT33564.1) (Figure 3B).

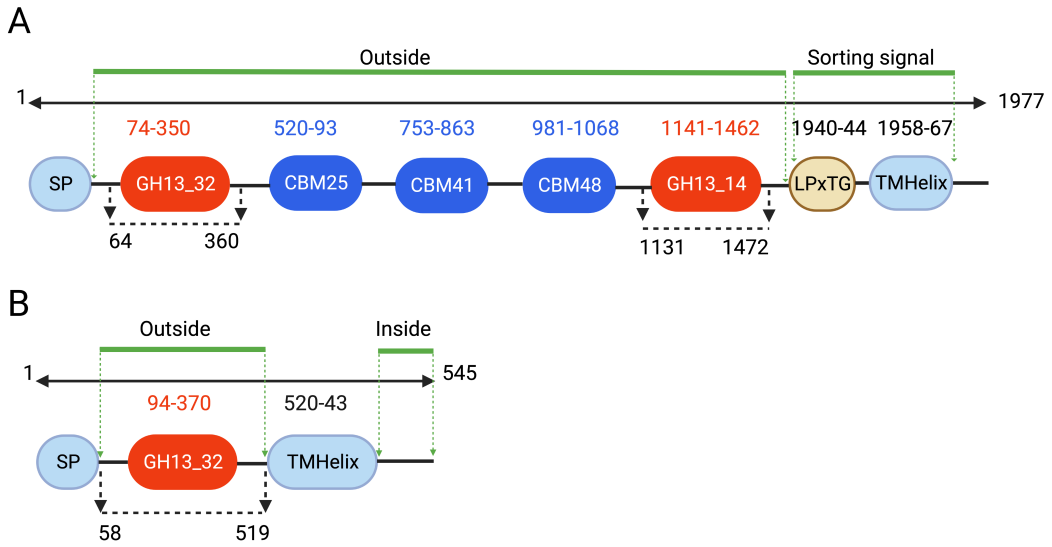

Figure 3: Predicted domains of *G. leopoldii* NR017 α-amylase-pullulanase (1977 amino acids) (A) and α-amylase (545 amino acids) (B). Amylase and pullulanase domains belonging to GH13 subfamilies 32 and 14 are indicated in red while three carbohydrate binding modules (CBM) are in blue. SP, Signal peptide; Sorting signal: LPxTG motif and a hydrophobic transmembrane helix domain (TMHelix) domain. Numbering indicates amino acid positions. The regions used for recombinant protein expression are indicated with black broken line with arrows. Predicted extracellular and intracellular regions are indicated with green lines.

Phylogenetic analysis of GH13_32 amylase domains and relationship with other amylases

GH13_32 amylase domain sequences from the single domain α-amylase and α-amylase-pullulanase from all study isolates formed two distinct clusters (Figure 4A). Intra-cluster amino acid sequence identity of amylase domains within single domain α-amylase and α-amylase-pullulanase enzymes was 75-100% and 66-100%, respectively, whereas inter-cluster identity was 64-74%.

GH13 enzymes have a conserved catalytic triad of two aspartate residues (acts as a nucleophile and to stabilize the transition state) and a glutamate residue (general acid base) (24). *In silico* analysis of GH13_32 amylase domains of *G. leopoldii* NR017 with GH13_32 amylase domains of functionally characterized α-amylase and α-amylase-pullulanase revealed conserved

catalytic residues (Figure 4B). The catalytic triad was conserved across all GH13_32 amylase domains from 15 *Gardnerella* isolates. (Supplementary Figure 1).

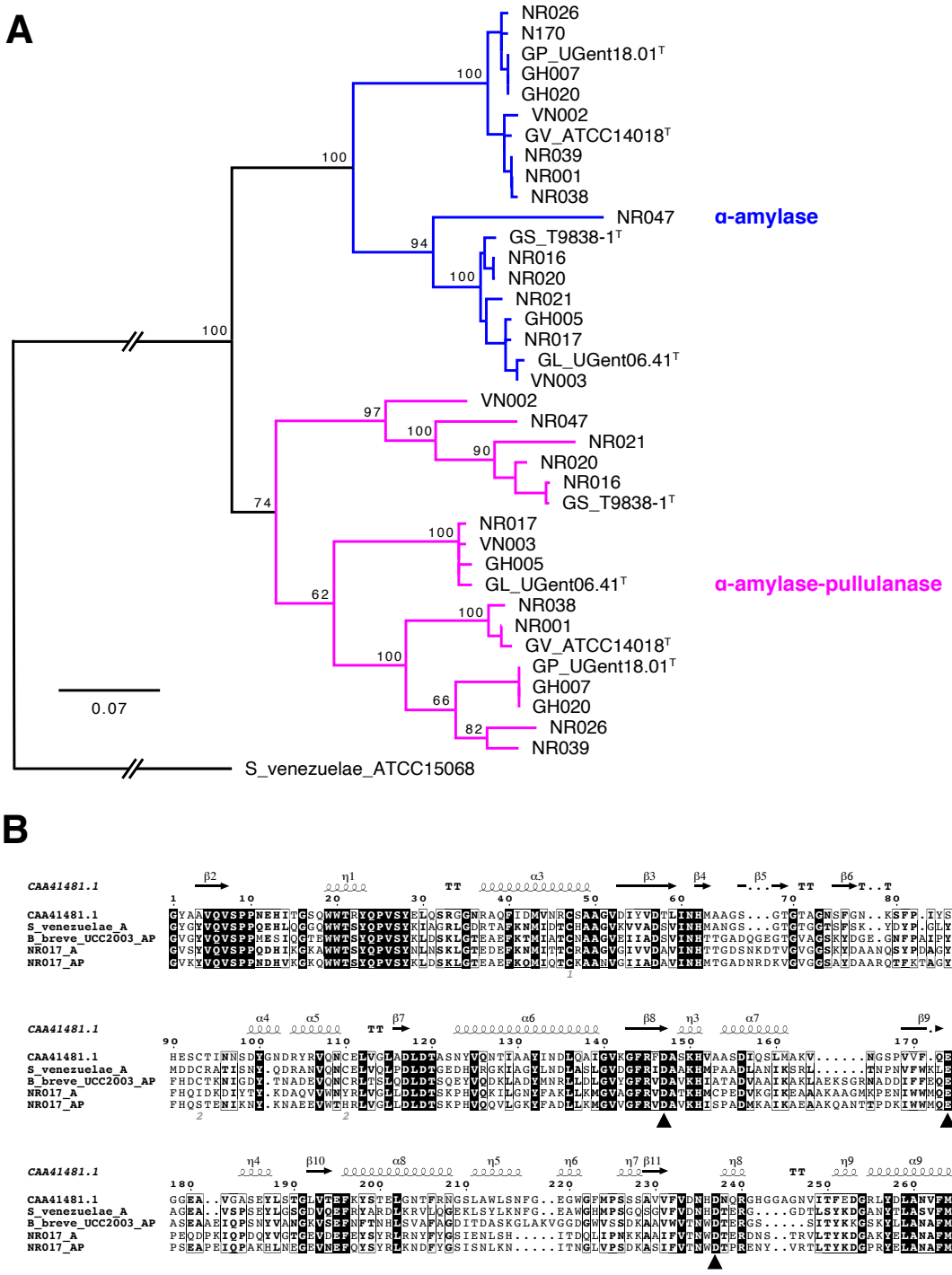

Figure 4: (A) Phylogenetic tree of all α-amylase domains from 15 *Gardnerella* isolates and 4 reference strains (indicated with T after the strain name). The tree is rooted with *Streptomyces venezuelae* ATCC15068. Trees are consensus trees of 100 bootstrap iterations and constructed

286 using Neighbour joining method using Tamura-Nei distance model. The number at major branch
287 points represents the percentage bootstrap support. (B) Sequence alignment of GH13_32 catalytic
288 domains of *G leopoldii* NR017 α-amylase (NR017_A) and α-amylase-pullulanase (NR017_AP)
289 with other functionally characterized GH13_32 members ((α-amylases from *Psuedoalternomonas*
290 *haloplanktis* A23 (CAA41481.4) and *S. venezuelae* ATCC15068) and 'amylopullulanase' from
291 *Bifidobacterium breve* UCC2003). Black triangles indicate conserved catalytic residues.

292

293 **Protein expression and purification**

294 The entire open reading frame of *G. leopoldii* NR017 α-amylase-pullulanase (GH13_32
295 and GH13_14) comprises 5,933 bp encoding a 1,977 amino acid protein with a predicted mass of
296 215.3 kDa (Figure 3A). The gene segments encoding the α-amylase (amino acids 64-360) and
297 pullulanase domains (amino acids 1131-1472) were each PCR amplified and ligated into pQE-
298 80L vector to express as N-terminal 6His-tagged proteins in *E. coli* (Figure 5A, left panel).
299 Expressed proteins were solubilized using 1% SDS and purified using nickel-nitriloacetic acid
300 (Ni-NTA) columns (Supplementary Figure 2). Apparent molecular weights of the 6His-tagged
301 amylase and pullulanase domains were 35.7 and 40.5 kDa, respectively (Figure 5B, left and
302 middle).

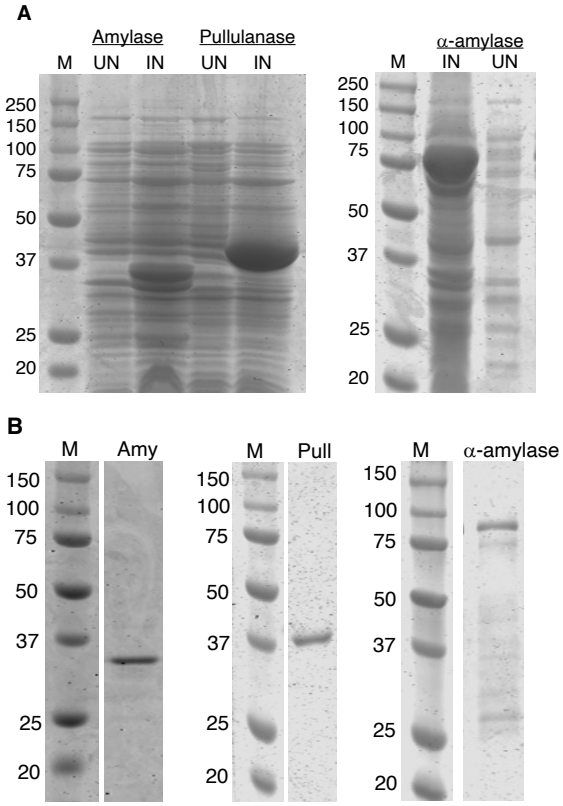

Figure 5: (A) Protein profiles of uninduced (UN) and induced (IN) *E. coli* cells containing pQE80L-AMY & pQE80L-PULL (top left) and pET41a+CO-AMY (top right) recombinant plasmids. (B) Purified 6His-tagged amylase (Amy) (bottom left) and pullulanase (Pull) (bottom middle) and GST-6His-tag α-amylase (bottom right). M molecular weight markers.

The *G. leopoldii* NR017 α-amylase enzyme (1635 bp encoding a 545 amino acid protein with a predicted mass of 60.5 kDa) has a predicted N-terminal signal peptide (amino acids 1-57) and C-terminal transmembrane domain (amino acids 520-545) (Figure 3B). A codon-optimized version of the truncated α-amylase gene sequence encoding amino acids 58-519 was expressed as a GST fusion protein with an apparent molecular weight of 79.9 kDa in *E. coli* BL21 DE3 cells (Figure 5A, right). The recombinant protein was solubilized using 1% SDS. Attempts to purify this GST fusion protein using glutathione beads resulted in a very low recovery of target protein due to poor binding to the beads (Supplementary Figure 3). The pET41a+amylase construct

317 includes an N-terminal hexa-histidine tag between the GST tag and the amylase sequence.
318 Purification of the fusion protein using a Ni-NTA column resulted in partial protein purification
319 (Figure 5B, right). Additional lower molecular weight peptides observed in the column eluate were
320 identified as degraded peptide fragments of the fusion protein by western blot with anti-His
321 antibodies (Supplementary Figure 4).

322 **Activity of the purified proteins**

323 The α-amylase domain from the α-amylase-pullulanase released maltose and maltotriose
324 from maltopentose while maltose, maltotriose and maltotetraose were identified as the major
325 products from maltodextrin (dextrose equivalent 13-17) and glycogen (Figure 6A). A small peak
326 corresponding to isomaltose was observed in the HPAEC-PAD results from 24 and 48 h digests
327 of glycogen with α-amylase domain (Figure 6A- middle right). The pullulanase domain produced
328 maltotriose as the only product from pullulan (Figure 6B) while maltose was produced from
329 glycogen (Figure 6C). Combined activities of the α-amylase and pullulanase domains on glycogen
330 released maltose and maltotriose (Figure 6C) with no detectable maltotetraose. This suggests that
331 the pullulanase domain can hydrolyze maltotetraose to release maltose but is less active (or
332 inactive) on the smaller maltotriose substrate, perhaps because it is a poorer fit for the active site.
333 To test this, the pullulanase domain was incubated with maltotriose, maltotetraose and
334 maltopentose. The results showed that pullulanase hydrolyzed maltopentose (into maltose and
335 maltotriose), and to a lesser extent, maltotetraose (into maltose) and maltotriose (into glucose and
336 maltose) (Supplementary Figure 6). Overall, our results show that α-amylase and pullulanase
337 domains from α-amylase-pullulanase can hydrolyse α-1,4, and α-1,4 and α-1,6 glycosidic bonds
338 in glycogen, respectively.

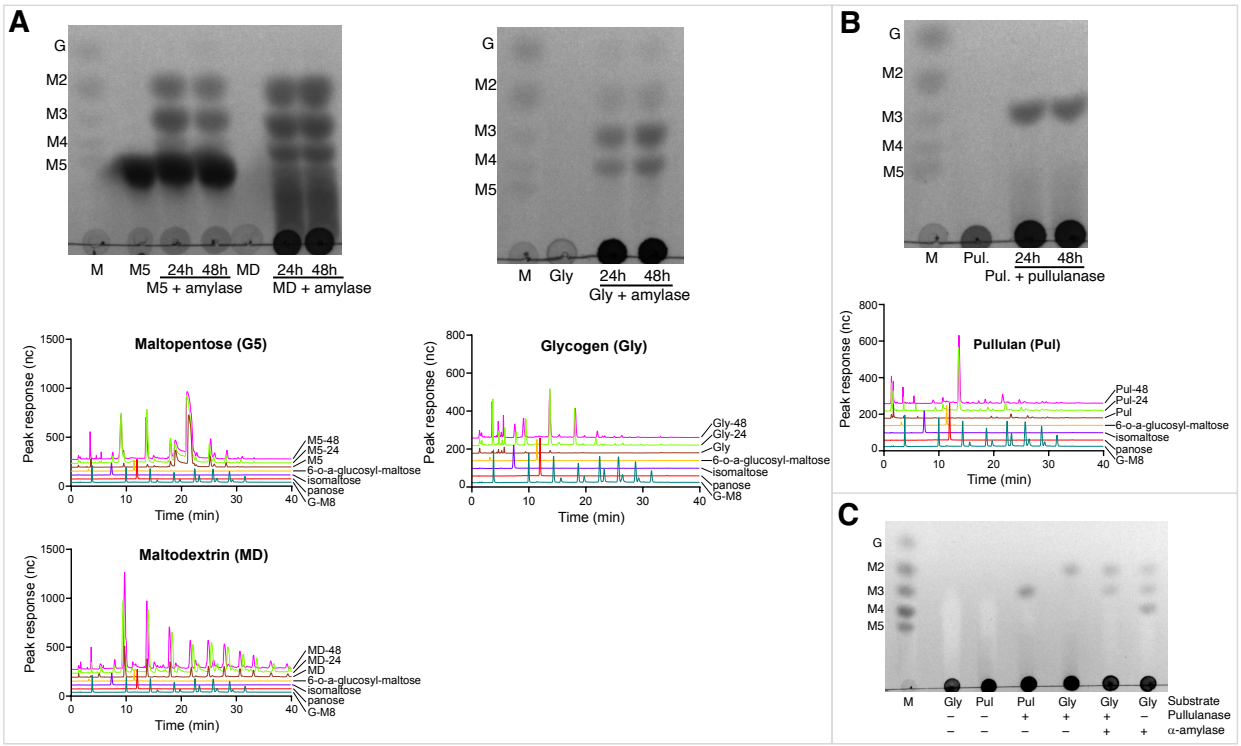

Figure 6: (A) Identification of products released by α-amylase domain (GH13_32) of α-amylase-pullulanase from maltopentose (M5) and maltodextrin (MD) and glycogen (Gly) after 24 and 48h of incubation using TLC (top) and HPAEC-PAD (middle and bottom). (B) Products released from pullulan by the pullulanase domain (GH13_14) after 24 and 48 h incubation were identified using TLC (top) and HPAEC-PAD (bottom). (C) Identification of products released after 24h from pullulan or glycogen by pullulanase, α-amylase or a mixture of α-amylase and pullulanase domains. Standards in Lane M of each panel: G: glucose, M2: maltose, M3: maltotriose, M4: maltotetraose and M5: maltopentose.

Since the α-amylase domain from the single-domain α-amylase enzyme was expressed as a GST-6xHis fusion, we initially confirmed that no amylase activity was detected from the GST-6xHis tag (Supplementary Figure 5). Maltose and maltotriose were produced when maltopentose was incubated with single domain α-amylase (Figure 7A, top and middle). Similarly, maltose, maltotriose and maltotetraose were identified as the major products in the reaction mixture of glycogen with single domain α-amylase (Figure 7B). As expected, the maltodextrin substrate included maltose, maltotriose and maltotetraose, however, an increase in intensity of maltose,

356 maltotriose and maltotetraose spots was observed in TLC results in the reaction mixture of single
357 domain α-amylase with maltodextrin when compared to a substrate only control (Figure 7A, top).
358 HPAEC-PAD analysis of products from maltodextrin also showed larger peaks of maltose,
359 maltotriose and maltotetraose relative to the control (Figure 7A, bottom).

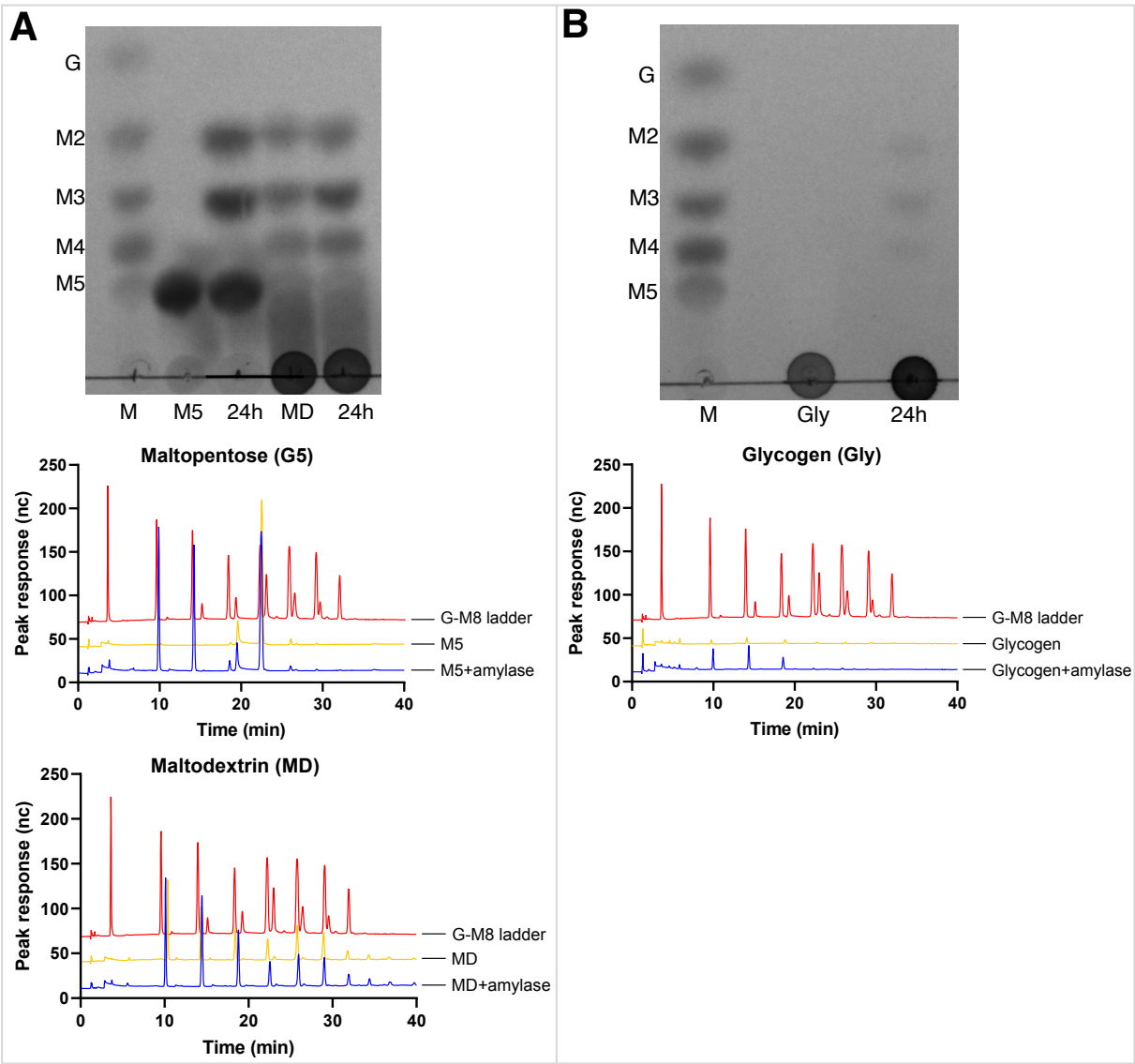

360

361 Figure 7: (A) Identification of products released by the purified single domain α-amylase enzyme
362 from maltopentose (M5) and maltodextrin (MD) using TLC (top) and HPAEC-PAD (bottom) after
363 24h incubation. (B) Products released from glycogen by the purified single domain α-amylase
364 enzyme after 24 h incubation were identified using TLC (top) and HPAEC-PAD (bottom).
365 Standards in Lane M of each panel: G: glucose, M2: maltose, M3: maltotriose, M4: maltotetraose
366 and M5: maltopentose.

367

368 **Discussion**

369 Dysbiosis in the vaginal microbiome has significant consequences that can affect the
370 quality of life and reproductive health of women. There are several hypotheses about how
371 dysbiosis is initiated and maintained (25, 26) but the ecological factors determining microbial
372 population dynamics in the vaginal microbiome are not well understood. In addition to direct
373 antagonistic (27) or synergistic (28) interactions among microbiota, changes in environmental
374 conditions due to pregnancy status, hormone levels, infection, sexual behaviour and hygiene
375 practices certainly play a role in determining the fitness of vaginal microbiota and thus microbial
376 community composition. *Gardnerella* spp. have been implicated in the initial stages of transition
377 to bacterial vaginosis (26) and so factors affecting their fitness, including their interaction with
378 vaginal glycogen, are of particular interest.

379 Glycogen breakdown is a complex and multistep process that requires the collective action
380 of several glycogen degrading enzymes. Vaginal secretions contain host derived pancreatic α-
381 amylase and α-glucosidases that can digest glycogen into smaller sugars (13). Until recently, the
382 contribution of bacterial enzymes in this process was unclear. Recently, van der Veer *et al.* showed
383 that vaginal isolates of *Lactobacillus crispatus* are capable of growing in glycogen supplemented
384 medium and encode type I pullulanase in their genomes (29). This study further reported that
385 strains showing less efficient or no growth on glycogen have an N-terminal deletion mutation in
386 their putative type I pullulanase gene suggesting its role in extracellular glycogen digestion. Forney
387 *et al.* identified eight putative amylases from vaginal metagenomes of *Bifidobacterium vaginale*,
388 *B. lacrimalis*, *L. gasseri*, *L. crispatus, L. iners* and *L. jensenni* and further reported that multiple
389 microbial amylases are present in vaginal fluid (14). Similarly, Woolston *et al.* identified putative

390 glycogen degrading enzymes in genomes of vaginal bacteria including *Gardnerella* spp. and
391 biochemically characterized the glycogen degradation ability of six GH13 hydrolase enzymes
392 (30) identified in those species. Together these findings suggest that bacterial enzymes contribute
393 to the breakdown of vaginal glycogen.

394 The genus *Gardnerella* was a mono-specific genus until recently when it was classified
395 into four species and additional "genome species" that have not yet been named due to insufficient
396 evidence (4). The role of *Gardnerella* spp. in extracellular glycogen digestion and whether the
397 species in this genus differ in digesting glycogen is not clear. Although earlier studies reported that
398 *Gardnerella* isolates can utilize glycogen (31–33), it is not clear if all newly defined species are
399 capable of digesting extracellular glycogen. In this study, we used cell free culture supernatants
400 from genetically characterized isolates to test extracellular glycogen breakdown ability of different
401 *Gardnerella* spp.

402 Selection of an appropriate culture medium to make culture supernatants is a challenge. As
403 our main interest was to identify the sugars released from glycogen, differentiating the background
404 sugars that are already present in medium from those obtained from glycogen hydrolysis is crucial.
405 *Gardnerella* is typically cultured in BHI broth or NYCIII and both media contain glucose. In
406 addition, the complement inactivated horse serum (obtained by heat treatment at 56ºC for 20
407 minutes) added to NYCIII can itself digest glycogen. It is reported that heat treatment at 70ºC for
408 20 minutes inhibits the maltase and amylase activity of fetal bovine serum but not horse serum
409 (34). For this reason, in our experiments a modified NYCIII media supplemented with heat
410 inactivated (70ºC for 20 minutes) fetal bovine serum instead of horse serum and no added glucose
411 was used to prepare culture supernatants. Cell free culture supernatants of all isolates tested
412 showed amylase activity in a glycogen agar plate assay, suggesting that glycogen degradation is a

413 conserved property in the genus *Gardnerella*. Glucose, maltose, maltotriose and maltotetraose
414 were identified as the major products released from glycogen by culture supernatants of all
415 *Gardnerella* isolates except N170 isolate which produced only glucose. Consistent with this
416 observation α-amylase-pullulanase genes were detected in all isolates except N170. Overall, no
417 species-specific patterns of glycogen breakdown products were found in *Gardnerella* spp.

418 Of the two extracellular glycosyl hydrolases identified by dbCAN2, the α-amylase-
419 pullulanase was predicted to contain separate amylase and pullulanase catalytic domains; a
420 conformation historically referred to as Type II amylopullulanase (35). With the availability of
421 more sequence data, these enzymes are now classified as Type II α-amylase-pullulanase and they
422 differ from amylopullulanases which have only one catalytic domain capable of hydrolyzing both
423 α-1,4 and α-1,6 glycosidic bonds (23). The amylase and pullulanase domains of the identified
424 *Gardnerella* α-amylase-pullulanase flanked 2 - 4 CBMs. CBMs appended to GH13 enzymes are
425 important for binding to different α-glucans, such as amylose, amylopectin, glycogen, pullulan
426 and oligosaccharides derived from these polysaccharides (36, 37). CBMs increase the
427 concentration of enzyme on the substrate surface and their removal can significantly reduce
428 enzyme activity. It is reported that removal of CBMs reduced the activity of *Eubacterium rectale*
429 α-amylase on starch by ~40 fold compared to the wildtype protein (38). Similarly, compared to a
430 full-length enzyme, removal of CBM domains reduced the activity of *B. adolescentis* P2P3 Type
431 II pullulanase on glycogen (39). We did not investigate the roles of the CBMs in the α-amylase-
432 pullulanase characterized in this study since our attempts to express full-length α-amylase-
433 pullulanase were unsuccessful.

434 Recently, Woolston *et al.* (30) characterized a full length 'amylopullulanase' (2013 amino
435 acids) from a vaginal isolate of *G. vaginalis* and reported maltose and maltotriose as the major

436 products from glycogen. In this report, the authors described the enzyme as containing 'α-amylase
437 domains' rather than amylase and pullulanase catalytic domains as we describe here. By
438 expressing the two catalytic domains separately we have demonstrated that they have distinct
439 activities, hydrolysing α-1,4, and α-1,4 and α-1,6 bonds, respectively.

440 Pullulanase degrading enzymes are classified into two major types, pullulanases (type I
441 and type II) and pullulanase hydrolases (type I, II and III) based on substrate specificities and
442 reaction products. While type I pullulanases hydrolyze only α-1,6 glycosidic bonds, type II
443 pullulanases are capable of hydrolyzing α-1,4 and α-1,6 glycosidic bonds. Amylopullulanase, a
444 subtype of type II pullulanase, are mainly reported in thermophilic bacteria and have a single
445 catalytic domain, whereas α-amylase-pullulanase has dual catalytic domains (α-amylase: for α-
446 1,4 glycosidic bonds and pullulanase: for α-1,6 glycosidic bonds) and are reported in mesophilic
447 bacteria (23). α-amylase-pullulanases have been characterized in *Bifidobacterium breve*
448 UCC2003, *B. adolescentis* P2P3 (39, 41) and a few other species (23). Our results showed that the
449 pullulanase domain of the *G. leopoldii* α-amylase-pullulanase hydrolyzes α-1,4 as well as α-1,6
450 glycosidic bonds, which to our knowledge has not been reported before. Kim *et al.* (2021) reported
451 that the pullulanase domain of an α-amylase-pullulanase from *B. adolescentis* P2P3 is capable of
452 hydrolyzing α-1,6 glycosidic bonds and releasing maltotriose from pullulan, however no products
453 were detected with amylose indicating a lack of activity on α-1,4 linkages (39). The demonstrated
454 activity of the *G. leopoldii* pullulanase domain on α-1,4, and α-1,6 glycosidic bonds would explain
455 why maltose was the only detectable product released from glycogen (Figure 6C) and suggests
456 that this domain might better be described as an amylopullulanase. It is important to note, however,
457 that the lack of CBMs associated with the domains we investigated in the current study could affect

458 their activity and the range of products released from different substrates and so further study of
459 the influence of CBMs is warranted.

460 Both α-amylase and α-amylase-pullulanase enzymes are active against oligosaccharides
461 and glycogen. Although the overall sequence identity between the two amylase domains
462 characterized in this study was only 64-74%, predicted catalytic residues were perfectly conserved
463 (Figure 4B). Either domain would thus be capable of acting on the malto-oligosaccharides
464 produced by the debranching activity of the pullulanase domain to generate glucose, maltose, and
465 other small oligosaccharides. This type of functional redundancy where two enzymes have similar
466 biochemical activities is common in bacteria (40).

467 The *Gardnerella* α-amylase and α-amylase-pullulanase are predicted to be extracellular
468 based on the presence of N-terminal signal peptides. The α-amylase contains a C-terminal
469 transmembrane helix, suggesting that the protein is inserted in the cell membrane. In the α-
470 amylase-pullulanase sequence an LPxTG motif was identified immediately N-terminal to the
471 predicted transmembrane helix (Figure 3A), suggesting this protein is anchored to the cell wall
472 through the sortase mechanism. The presence of these features suggests that both enzymes are
473 tethered to the cell envelope. Cell envelope anchored proteins can be released into the extracellular
474 environment during bacterial growth as a by-product of cell wall turnover or cell death or
475 proteolytic cleavage (42), which is consistent with our detection of amylase activity in sterile
476 culture supernatants. Some *Gardnerella* species also produce cell wall anchored sialidases, NanH2
477 and NanH3, that are also released into the supernatant after cell death or by proteolytic cleavage
478 (43).

479 Although glucose was identified as one of the major products in glycogen digests of
480 *Gardnerella* culture supernatants, the purified α-amylase domain and single domain α-amylase

481 proteins did not produce glucose from glycogen. TLC and HPAEC-PAD analysis showed that
482 glucose was neither produced by the activity of culture media itself nor present in glycogen
483 substrate (Figure 2F& 2G). Another possibility is that the activity of a full-length α-amylase-
484 pullulanase protein on glycogen might generate different product profiles than the isolated
485 domains. A full-length type II pullulanase enzyme (containing two separate α-amylase and
486 pullulanase domains) from *Bifidobacterium adolescentis* P2P3 was reported to produce maltose
487 only from glycogen, while the purified amylase domain protein from the same enzyme produced
488 a mixture of glucose, maltose and maltotriose (39). Glucose may also be produced by the activity
489 of intracellular α-glucosidase on malto-oligosaccharides generated from glycogen hydrolysis that
490 are released by dead/lysed bacteria in the culture. We have previously shown that *Gardnerella* spp.
491 have conserved intracellular α-glucosidase that can release glucose from smaller oligosaccharides
492 (44).

493 Our findings show that all *Gardnerella* species produce extracellular α-amylase and α-
494 amylase-pullulanase enzymes that are 'public goods' in the vaginal microbiome, breaking down
495 glycogen to produce similar fingerprints of glycogen derived products and contributing to the
496 nutrient pool available to the vaginal microbiota (Figure 8). Determining if these *Gardnerella* spp.
497 differentially utilize and compete for these breakdown products will provide insights into whether
498 competition for malto-oligosaccharides plays a role in determining *Gardnerella* community
499 structure in the vaginal microbiome.

500

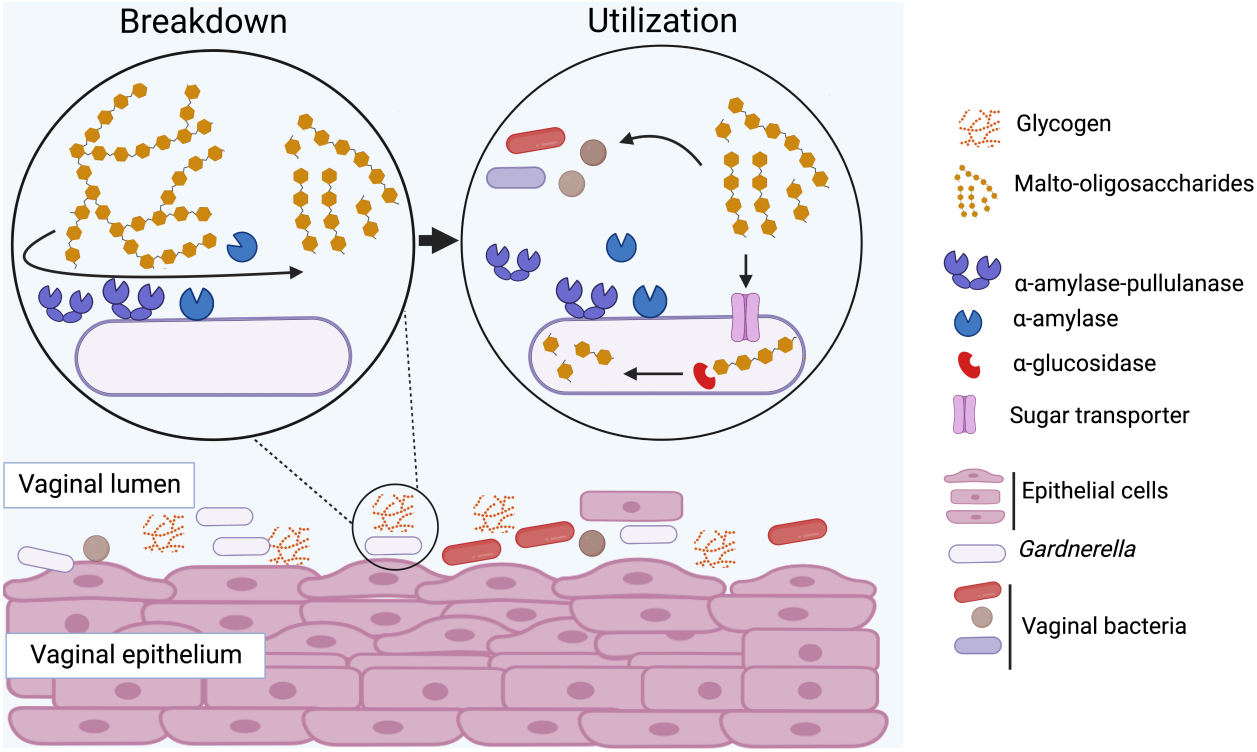

Figure 8: Proposed mechanisms of extracellular glycogen utilization in *Gardnerella* spp. Glycogen is digested into malto-oligosaccharides by α-amylase-pullulanase and α-amylase and these breakdown products are transported inside and can be further digested to glucose by other glycosyl hydrolases including a previously characterized α-glucosidase enzyme (44). Extracellular glycogen breakdown products can also be utilized by other resident microbiota.

Acknowledgements:

This research was supported by a Natural Sciences and Engineering Research Council of Canada Discovery Grant (J.E.H.) and Agriculture and Agri-Food Canada (D.W.A. project no. J-002262). P.B. is supported by a Devolved Scholarship from the University of Saskatchewan. The authors would like to thank Champika Fernando for technical support, Shubham Dutta for guidance with Western blot, and Noreen Rapin and Dr. Tony Ruzzini for providing reagents.

516 **References**

517 1. Hillier SL. 1993. Diagnostic microbiology of bacterial vaginosis. Am J Obstet Gynecol
518 169:455–459.

519 2. Muzny CA, Schwebke JR. 2020. Asymptomatic bacterial vaginosis: to treat or not to treat?
520 Curr Infect Dis Rep 22:32.

521 3. van de Wijgert JHHM, Borgdorff H, Verhelst R, Crucitti T, Francis S, Verstraelen H,
522 Jespers V. 2014. The vaginal microbiota: what have we learned after a decade of molecular
523 characterization? PLoS ONE 9:e105998.

524 4. Vaneechoutte M, Guschin A, Van Simaey L, Gansemans Y, Van Nieuwerburgh F, Cools P.
525 2019. Emended description of *Gardnerella vaginalis* and description of *Gardnerella*
526 *leopoldii* sp. nov., *Gardnerella piotii* sp. nov. and *Gardnerella swidsinskii* sp. nov., with
527 delineation of 13 genomic species within the genus *Gardnerella*. Int J Syst Evol Microbiol
528 69:679–687.

529 5. Hill JE, Albert AYK. 2019. Resolution and cooccurrence patterns of *Gardnerella leopoldii*,
530 *G. swidsinskii*, *G. piotii*, and *G. vaginalis* within the vaginal microbiome. Infect Immun
531 87:e00532-19.

532 6. Khan S, Voordouw MJ, Hill JE. 2019. Competition among *Gardnerella* subgroups from the
533 human vaginal microbiome. Front Cell Infect Microbiol 9:374.

534 7. Hibbing ME, Fuqua C, Parsek MR, Peterson SB. 2010. Bacterial competition: surviving
535 and thriving in the microbial jungle. Nat Rev Microbiol 8:15–25.

536 8. Adeva-Andany MM, González-Lucán M, Donapetry-García C, Fernández-Fernández C,
537 Ameneiros-Rodríguez E. 2016. Glycogen metabolism in humans. BBA Clin 5:85–100.

538 9. Cruickshank R, Sharman A. 1934. The biology of the vagina in the human subject. BJOG
539 Int J Obstet Gynaecol 41:208–226.

540 10. Nasioudis D, Beghini J, Bongiovanni AM, Giraldo PC, Linhares IM, Witkin SS. 2015. α-
541 amylase in vaginal fluid: association with conditions favorable to dominance of
542 *Lactobacillus*. Reprod Sci 22:1393–1398.

543 11. Mirmonsef P, Hotton AL, Gilbert D, Gioia CJ, Maric D, Hope TJ, Landay AL, Spear GT.
544 2016. Glycogen levels in undiluted genital fluid and their relationship to vaginal pH,
545 estrogen, and progesterone. PloS One 11:e0153553.

546 12. Lombard V, Golaconda Ramulu H, Drula E, Coutinho PM, Henrissat B. 2014. The
547 carbohydrate-active enzymes database (CAZy) in 2013. Nucleic Acids Res 42:D490–D495.

548 13. Spear GT, French AL, Gilbert D, Zariffard MR, Mirmonsef P, Sullivan TH, Spear WW,
549 Landay A, Micci S, Lee B-H, Hamaker BR. 2014. Human α-amylase present in lower-
550 genital-tract mucosal fluid processes glycogen to support vaginal colonization by
551 *Lactobacillus*. J Infect Dis 210:1019–1028.

552 14. Nunn KL, Clair GC, Adkins JN, Engbrecht K, Fillmore T, Forney LJ. 2020. Amylases in
553 the human vagina. mSphere 5:e00943-20.

554 15. Schellenberg JJ, Paramel Jayaprakash T, Withana Gamage N, Patterson MH, Vaneechoutte
555 M, Hill JE. 2016. *Gardnerella vaginalis* subgroups defined by cpn60 sequencing and
556 Sialidase activity in isolates from Canada, Belgium and Kenya. PloS One 11:e0146510.

557 16. Ryan SM, Fitzgerald GF, van Sinderen D. 2006. Screening for and identification of starch-,
558 amylopectin-, and pullulan-degrading activities in Bifidobacterial Strains. Appl Environ
559 Microbiol 72:5289.

560 17. Cockburn D, Koropatkin N. 2015. Product analysis of starch active enzymes by TLC.
561 Bioprotocol 5:1–8.

562 18. Zhang H, Yohe T, Huang L, Entwistle S, Wu P, Yang Z, Busk PK, Xu Y, Yin Y. 2018.
563 dbCAN2: a meta server for automated carbohydrate-active enzyme annotation. Nucleic
564 Acids Res 46:W95–W101.

565 19. Krogh A, Larsson B, von Heijne G, Sonnhammer ELL. 2001. Predicting transmembrane
566 protein topology with a hidden markov model: application to complete genomes11Edited
567 by F. Cohen. J Mol Biol 305:567–580.

568 20. Zhou M, Boekhorst J, Francke C, Siezen RJ. 2008. LocateP: Genome-scale subcellular-
569 location predictor for bacterial proteins. BMC Bioinformatics 9:173.

570 21. Robert X, Gouet P. 2014. Deciphering key features in protein structures with the new
571 ENDscript server. Nucleic Acids Res 42:W320–W324.

572 22. Schlager B, Straessle A, Hafen E. 2012. Use of anionic denaturing detergents to purify
573 insoluble proteins after overexpression. BMC Biotechnol 12:95.

574 23. Kahar UM, Latif NA, Amran SI, Liew KJ, Goh KM. 2022. A bibliometric analysis and
575 review of pullulan-degrading enzymes—past and current trends. Catalysts 12:143.

576 24. Uitdehaag JCM, Mosi R, Kalk KH, van der Veen BA, Dijkhuizen L, Withers SG, Dijkstra
577 BW. 1999. X-ray structures along the reaction pathway of cyclodextrin glycosyltransferase
578 elucidate catalysis in the α-amylase family. Nat Struct Biol 6:432–436.

579 25. Muzny CA, Schwebke JR. 2016. Pathogenesis of bacterial vaginosis: discussion of current
580 hypotheses. J Infect Dis 214:S1–S5.

581 26. Muzny CA, Taylor CM, Swords WE, Tamhane A, Chattopadhyay D, Cerca N, Schwebke
582 JR. 2019. An updated conceptual model on the pathogenesis of bacterial vaginosis. J Infect
583 Dis 220:1399–1405.

584 27. Atassi F, Brassart D, Grob P, Graf F, Servin AL. 2006. *Lactobacillus* strains isolated from
585 the vaginal microbiota of healthy women inhibit *Prevotella bivia* and *Gardnerella vaginalis*
586 in coculture and cell culture. FEMS Immunol Med Microbiol 48:424–432.

587 28. Castro J, Rosca AS, Cools P, Vaneechoutte M, Cerca N. 2020. *Gardnerella vaginalis*
588 enhances *Atopobium vaginae* viability in an in vitro model. Front Cell Infect Microbiol
589 10:83.

590 29. van der Veer C, Hertzberger RY, Bruisten SM, Tytgat HLP, Swanenburg J, de Kat
591 Angelino-Bart A, Schuren F, Molenaar D, Reid G, de Vries H, Kort R. 2019. Comparative
592 genomics of human *Lactobacillus crispatus* isolates reveals genes for glycosylation and
593 glycogen degradation: implications for in vivo dominance of the vaginal microbiota.
594 Microbiome 7:49.

595 30. Woolston BM, Jenkins DJ, Hood-Pishchany MI, Nahoum SR, Balskus EP. 2021.
596 Characterization of vaginal microbial enzymes identifies amylopullulanases that support
597 growth of *Lactobacillus crispatus* on glycogen. preprint. Biochemistry.

598 31. Edmunds PN. 1962. The biochemical, serological and haemagglutinating reactions of
599 *Haemophilus vaginalis*. J Pathol Bacteriol 83:411–422.

600 32. Piot P, Van Dyck E, Totten PA, Holmes KK. 1982. Identification of *Gardnerella*
601 (*Haemophilus*) *vaginalis*. J Clin Microbiol 15:19–24.

602 33. Dunkelberg WE, McVeigh I. 1969. Growth requirements of *Haemophilus vaginalis*.
603 Antonie Van Leeuwenhoek 35:129–145.

604 34. Huffman RD, Nawrocki LD, Wilson WA, Brittingham A. 2015. Digestion of glycogen by
605 α-glucosidase released by *Trichomonas vaginalis*. Exp Parasitol 159:151–159.

606 35. Hii SL, Tan JS, Ling TC, Ariff AB. 2012. Pullulanase: role in starch hydrolysis and
607 potential industrial applications. Enzyme Res 2012:1–14.

608 36. Boraston AB, Healey M, Klassen J, Ficko-Blean E, van Bueren AL, Law V. 2006. A
609 structural and functional analysis of α-glucan recognition by family 25 and 26
610 carbohydrate-binding modules reveals a conserved mode of starch recognition. J Biol Chem
611 281:587–598.

612 37. Cantarel BL, Coutinho PM, Rancurel C, Bernard T, Lombard V, Henrissat B. 2009. The
613 Carbohydrate-Active EnZymes database (CAZy): an expert resource for glycogenomics.
614 Nucleic Acids Res 37:D233–D238.

615 38. Cockburn DW, Suh C, Medina KP, Duvall RM, Wawrzak Z, Henrissat B, Koropatkin NM.
616 2018. Novel carbohydrate binding modules in the surface anchored α-amylase of
617 *Eubacterium rectale* provide a molecular rationale for the range of starches used by this
618 organism in the human gut. Mol Microbiol 107:249–264.

619 39. Kim S-Y, Kim H, Kim Y-J, Jung D-H, Seo D-H, Jung J-H, Park C-S. 2021. Enzymatic
620 analysis of truncation mutants of a type II pullulanase from *Bifidobacterium adolescentis*
621 P2P3, a resistant starch-degrading gut bacterium. Int J Biol Macromol 193:1340–1349.

622 40. Ghosh S, O'Connor TJ. 2017. Beyond paralogs: the multiple layers of redundancy in
623 bacterial pathogenesis. Front Cell Infect Microbiol 7:467.

624 41. O'Connell Motherway M, Fitzgerald GF, Neirynck S, Ryan S, Steidler L, van Sinderen D.
625 2008. Characterization of *ApuB*, an extracellular type II amylopullulanase from
626 *Bifidobacterium breve* UCC2003. Appl Environ Microbiol 74:6271–6279.

627 42. Siegel SD, Reardon ME, Ton-That H. 2016. Anchoring of LPXTG-like proteins to the
628 gram-positive cell wall envelope, p. 159–175. *In* Bagnoli, F, Rappuoli, R (eds.), Protein and
629 Sugar Export and Assembly in Gram-positive Bacteria. Springer International Publishing,
630 Cham.

631 43. Agarwal K, Lewis AL. 2021. Vaginal sialoglycan foraging by *Gardnerella vaginalis* :
632 mucus barriers as a meal for unwelcome guests? Glycobiology 31:667–680.

633 44. Bhandari P, Tingley JP, Palmer DRJ, Abbott DW, Hill JE. 2021. Characterization of an α-
634 glucosidase enzyme conserved in *Gardnerella* spp. isolated from the human vaginal
635 microbiome. J Bacteriol 203(17): e00213-21.